

# ADAPTIVE FUZZY-HYSTERESIS BAND CURRENT CONTROLLER FOR FOUR-WIRE SHUNT ACTIVE FILTER

F. Hamoudi\*, A. Chaghi\*, M. Adli\*\*, H. Amimeur\*, E. Merabet\*

\*Department of Electrical Engineering, University of Batna. Street Chahid Mohamed El hadi Boukhrouf, 05000, Batna, Algeria (email : f\_hamoudi@yahoo.fr; az\_chaghi@yahoo.fr; amimeurhocine@yahoo.fr; merabet\_elkheir@yahoo.fr).

\*\*Department of Electrical Engineering, University of Bejaia. Street of Targa ouzamour, 06000, Bejaia, Algeria (email : mulud.adli@yahoo.fr).

**Abstract:** This paper presents an adaptive Fuzzy-hysteresis band current controller for four-wire shunt active power filters, to eliminate harmonics and to compensate reactive power in distribution systems, in order to keep currents at the point of common coupling sinusoidal and in phase with the corresponding voltage and the cancel neutral current. The conventional hysteresis band controller, known for its robustness and its advantage in current controlled applications is adapted with a fuzzy logic controller, to change the bandwidth according to the operating point in order to keep the frequency modulation at tolerable limits. The algorithm used to identify the reference currents is based on the synchronous reference frame theory ( $dq\gamma$ ), considering disturbed network voltage. Finally, simulation results using Matlab/Simulink are given and compared with some Proportional-Integral control results, to measure and to validate the performances of proposed control.

**Key words:** Four-wires shunt active filter, Synchronous reference frame, Fuzzy-hysteresis band control, PI control.

## 1. Introduction

Active filters have come into view around 1970, after that, the concept has been successfully developed, tested and assisted by the power electronics technology, and put in practical uses. In term of topology, three-phase filters can be divided into three-wire and four-wire active filters [1-11]. The first one is well-developed and put in industrial applications, however, in last years, researches are more oriented to the second one for its advantage in four-wire distribution systems [6-8].

In this paper the four-wires three-phase shunt active filter for current compensation, using the conventional voltage three legs source inverter as illustrated in Fig 1 is studied.

The active filter control can be divided into two different parts; the first is the algorithm used to identify the suitable currents to be injected in the network to achieve compensation objectives, while the second part is the current control or regulation, which forces the shunt active filter to synthesize the desired current with minimized error. For this part, many kinds of technics are used as PI controller [9-10], RST controller [11], with PWM modulation, or hysteresis controller, this last one is very suitable for several reasons such as: simplicity, easy implementation, very fast response and good accuracy. However, the hysteresis band current control presents an undesirable feature in its high commutation frequency, which varies with the operating point. From the theoretical point of view, increasing switching frequency permits a very good reproduction of the reference currents especially in harmonics current control, but

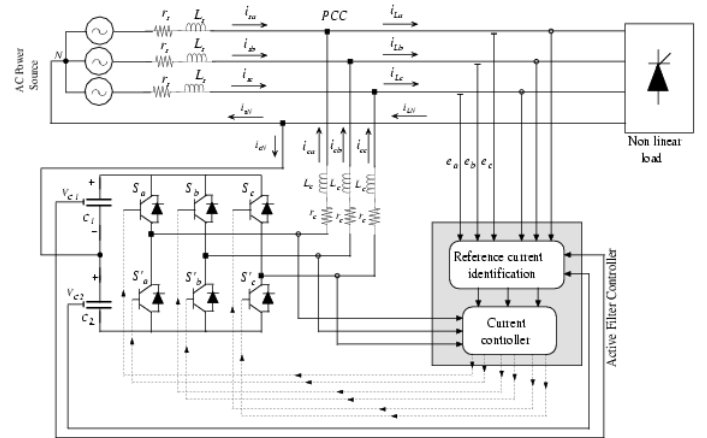


Fig.1. Configuration of the four-wires shunt active filter.

in practical uses, this frequency is limited by the nature of the semi-conductors and the passive elements.

This paper focuses on the idea of compromising between the robustness of an hysteresis controller and the constraint due to the stability of switching frequency. For this, a Fuzzy-hysteresis controller is proposed; the role of the Fuzzy-controller is to adapt the hysteresis bandwidth following the operating point, thus, the switching frequency is keep almost constant at predefined value.

The layout of this paper is as follows: first, we have presented briefly the four wires active filter configuration and the reference current identification based on the synchronous reference frame. Next, the adaptive Fuzzy-hysteresis band current controller is described. Finally, simulation results are given putting the accent on the comparison with some simulation results obtained with a conventional Proportional-Integral controller, followed by the conclusion.

## 2. Four-Wire Shunt Active Filter

The general configuration of the four wires shunt active filter presented in this paper is shown in Fig 1. The DC bus is constituted of two capacitors  $C_1 = C_2 = C$  with a midpoint connected to the neutral wire of the network. The AC side of the active filter is connected to the network through a first order passive inductive filter. This topology permits to compensate not only phase currents but also to cancel the neutral current. The model of the three-leg four-wire voltage source inverter (1) permits to show that the output voltage of the  $k$ -leg depend only of the switching function  $d_k$  ( $k = a, b, c$ ) of the same leg, this

mean that this topology can be assimilated to three decoupled single phase active filter.

$$v_k = d_k V_{C1} - \bar{d}_k V_{C2} \quad (1)$$

The interaction between the shunt active filter and the network can be described by the following state equation (2).

$$[\dot{X}] = [A][X] + [B] \quad (2)$$

Where;

$$A = \begin{bmatrix} -\frac{r_c}{L_c} & 0 & 0 & \frac{d_a}{L_c} & -\frac{\bar{d}_a}{L_c} \\ 0 & -\frac{r_c}{L_c} & 0 & \frac{d_b}{L_c} & -\frac{\bar{d}_b}{L_c} \\ 0 & 0 & -\frac{r_c}{L_c} & \frac{d_c}{L_c} & -\frac{\bar{d}_c}{L_c} \\ -\frac{d_a}{C} & -\frac{d_b}{C} & -\frac{d_c}{C} & 0 & 0 \\ \frac{d_a}{C} & \frac{d_b}{C} & \frac{d_c}{C} & 0 & 0 \end{bmatrix},$$

$$X = \begin{bmatrix} i_{ca} \\ i_{cb} \\ i_{cc} \\ V_{C1} \\ V_{C2} \end{bmatrix}, \text{ and } B = \begin{bmatrix} \frac{e_a}{L_c} \\ \frac{e_b}{L_c} \\ \frac{e_c}{L_c} \\ 0 \\ 0 \end{bmatrix}$$

With  $e_a, e_b$  and  $e_c$  are the network voltages at the point of common coupling;

$i_{ca}, i_{cb}, i_{cc}$  are the compensating currents;

$r_c, L_c$  are respectively, the resistance and the inductance of the coupling passive filter.

### 3. Reference Currents Identification

The synchronous reference frame used to identify the reference compensating currents consists to transform the instantaneous load currents  $i_{Lk}$  in a turn coordinate system by using Park transformation, in order to make easy the separation of the undesired components from the measured currents [12].

$$\begin{bmatrix} i_{Ld} \\ i_{Lq} \\ i_{L\gamma} \end{bmatrix} = \sqrt{\frac{2}{3}} \cdot T(\hat{\theta}) \begin{bmatrix} i_{La} \\ i_{Lb} \\ i_{Lc} \end{bmatrix} \quad (3)$$

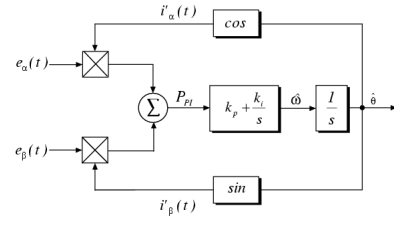
Where;

$$T(\hat{\theta}) = \begin{bmatrix} \cos(\hat{\theta}) & \cos(\hat{\theta} - 2\pi/3) & \cos(\hat{\theta} - 4\pi/3) \\ -\sin(\hat{\theta}) & -\sin(\hat{\theta} - 2\pi/3) & -\sin(\hat{\theta} - 4\pi/3) \\ 1/\sqrt{2} & 1/\sqrt{2} & 1/\sqrt{2} \end{bmatrix}$$

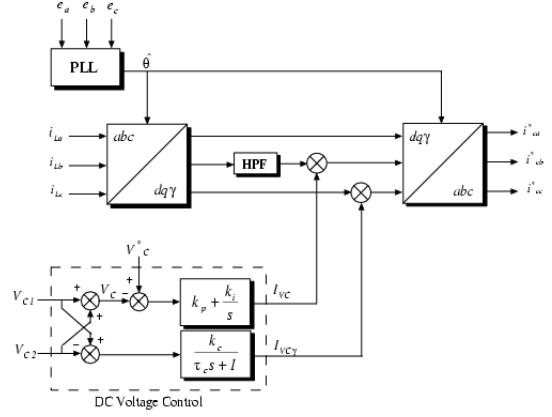
In fact, if the rotating angle  $\hat{\theta}$  correspond to the fundamental frequency, then currents in  $dq\gamma$ -axis are composed by a DC component (related with fundamentals) and AC components (with harmonics), which can be separated easily by using high-pass filter.

$$\begin{aligned} i_{Ld} &= \bar{i}_{Ld} + \tilde{i}_{Ld} \\ i_{Lq} &= \bar{i}_{Lq} + \tilde{i}_{Lq} \\ i_{L\gamma} &= \bar{i}_{L\gamma} + \tilde{i}_{L\gamma} \end{aligned} \quad (4)$$

Note that  $i_{Ld}$  correspond to the reactive power,  $i_{Lq}$  correspond to the active power and  $i_{L\gamma}$  to the homopolar power flowing through the neutral wire.



(a) PLL system



(b) Compensating current identification.

Fig.2. Complete Block diagram of the reference current identification.

In general, the rotating angle  $\hat{\theta}$  used in the Park transformation is given by a Phase Locked loop (PLL) since network voltages.

#### 3.1. PLL System

The PLL system used to extract the instantaneous fundamental angle  $\hat{\theta}$  is shown in Fig 2(a), it is based on the  $pq$ -theory [13]. The instantaneous real power in the PI-controller input is:

$$p_{PI} = e_\alpha i'_\alpha + e_\beta i'_\beta \quad (5)$$

Where  $e_\alpha$  and  $e_\beta$  are the measured voltages transformed in  $(\alpha, \beta)$  coordinate, and the feedback signals  $i'_\alpha, i'_\beta$  are the cosine and the sine of the angle at the PLL circuit.

This circuit can reach the stable point of operation only if the output  $p_{PI}$  of the PI-controller has zero average value ( $\bar{p}_{PI}=0$ ) and minimized alternative value ( $\bar{p}_{PI} \approx 0$ ). Otherwise, the average power in three-phase system is given by:

$$P_{avg} = 3E_1^+ I_1^+ \cos(\phi_{E1^+} - \phi_{I1^+}) \quad (6)$$

This means that the stable point of operation is found only  $\hat{\omega}$  correspond to the fundamental frequency of the system and the auxiliary signals  $i'_\alpha$  and  $i'_\beta$  become orthogonal to the measured network voltages  $e_\alpha$  and  $e_\beta$  respectively.

#### 3.2. DC Voltage Regulation

It is well known that the voltage of the DC bus should be maintained at a predefined design value to achieve correctly the compensation. As a particular characteristic for four-wire three-leg active filter is that the DC voltage regulation is constituted of two control loops; the first loop keeps the voltage  $V_C = V_{C1} + V_{C2}$  constant around its reference  $V_C^*$ . This is achieved by a PI-controller, which generate an active current  $I_{VC}$  added to the active filter reference current in order to inject or to absorb an additional active current in or from the network, which keeps  $V_C$  constant. The second loop permits to balance the voltages  $V_{C1}$  and  $V_{C2}$ , for this, the deference  $I_{VC\gamma} = V_{C1} - V_{C2}$  is added through a low pass filter as an

homopolar current in the active filter reference current with the same effect as the regulation [8].

### 3.3. Reference Current calculus

The reference compensating currents are calculated by the non desired parts of the currents  $i_{Ld}$ ,  $i_{Lq}$  and  $i_{L\gamma}$  to achieve compensation objectives, if we want to compensate exclusively harmonics, then  $\tilde{i}_{Ld}$ ,  $\tilde{i}_{Lq}$  and  $\tilde{i}_{L\gamma}$  are used to calculate reference compensating currents, but in general the fundamental reactive power should be compensated. In this case, the *DC* part of  $i_{Ld}$  is included, therefore, the reference compensating current are given in the *abc*-coordinate using the inverse Park transformation.

$$\begin{bmatrix} i_{ca}^* \\ i_{cb}^* \\ i_{cc}^* \end{bmatrix} = \sqrt{\frac{2}{3}} \cdot T^{-1}(\hat{\theta}) \begin{bmatrix} i_{Ld} \\ \tilde{i}_{Lq} + I_{VC} \\ i_{L\gamma} + I_{VC\gamma} \end{bmatrix} \quad (7)$$

Finally, the complete block diagram of the compensating current identification is illustrated in Fig 2.

### 4. PI Current Control

The conventional PI control is the most classically used for the current control applications [9-10][14], it is used often with a PWM modulator as shown in Fig 3.

The proportional  $K_p$  and integrator  $K_i$  gains of the PI controller are in general chosen from the closed transfer function of the system (active filter+PI controller);

$$H_{CL} = \frac{k_p s + k_i}{L_c s^2 + (r_c + k_p) s + k_i} \quad (8)$$

Which can be rewritten as:

$$H_{CL} = \frac{(2\xi\omega_c - \frac{r_c}{L_c})s + \omega_c^2}{s^2 + 2\xi\omega_c s + \omega_c^2} \quad (9)$$

For a good dynamic response,  $\xi$  is generally chosen equal to 0.7. Otherwise, for a maximal reject of harmonic due to the commutation, the cut pulsation  $\omega_c$  must be distant as much that possible of the pulsation of commutation of the PWM frequency.

If this kind of control is known for its simplicity, it is important to note that it is not an adequate solution to control multi-frequency signals. In fact, it is easy to show from the frequency analysis of (9), that this controller cannot with perfect fidelity (module  $\langle H_{CL}(jw) \rangle = 1$ , and argument  $\widehat{H_{CL}}(jw) = 0$ ) high frequency references [10][14]. This is an important handicap for harmonic compensation. Some authors preconize the use of PI-controllers in multi-turn frames, each one is turning in synchronism with the frequency which will be eliminated [10][14], but this solution require an important effort of calculus.

### 4. The Adaptive Fuzzy Hysteresis Band Current Controller

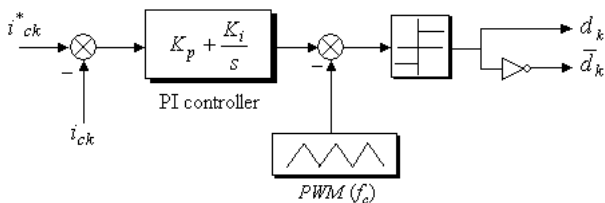


Fig.3. PI inverter current control scheme.

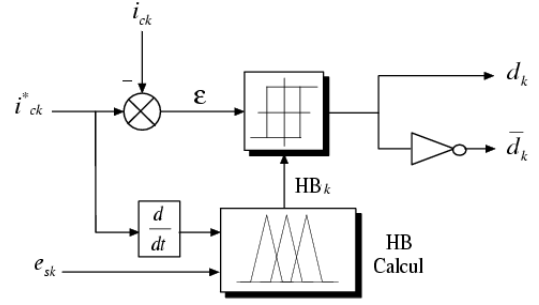


Fig.4. The adaptive Fuzzy-hysteresis band current controller.

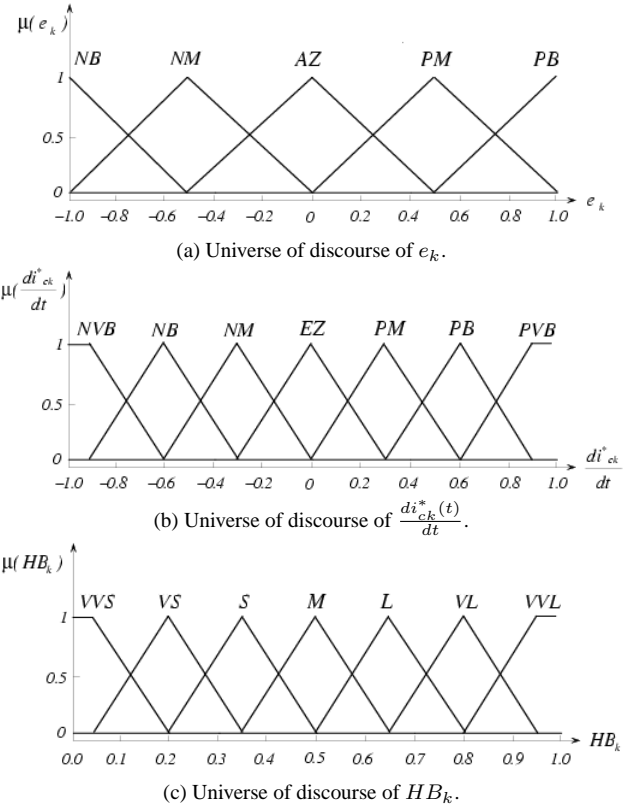


Fig.5. Universes of discourse for the inputs and output variables.

As it was mentioned in the introduction, the hysteresis band current control technique presents very good characteristics for current control applications. In the case of a voltage source inverter with a midpoint in the DC bus the width of the hysteresis band  $HB_k$  is given for each phase in [15] by:

$$HB_k = \frac{V_{DC}}{8f_m L_c} \left[ 1 - \frac{4L_c^2}{V_{DC}^2} \left( \frac{e_k(t)}{L_c} + \frac{di_{ck}^*(t)}{dt} \right) \right] \quad (10)$$

Where  $f_m$  is the modulation frequency,  $\frac{di_{ck}^*(t)}{dt}$  is the slope of the reference current for the  $k$ -phase,  $e_k$  is the instantaneous voltage at the common coupling point of the same phase,  $L_c$  and  $V_c$  are respectively the decoupling inductance and the DC bus voltage.

Regarding the equation (10), we can remark that in order to keep the modulation frequency  $f_m$  constant it is necessary to regulate the bandwidth  $HB_k$  at different operating points, following the variations of the different parameters in (10).

Table.1. Fuzzy rules for the hysteresis bandwidth.

$HB_k$		$e_k$				
		$NB$	$NM$	$AZ$	$PM$	$PB$
$di_{ck}^*/dt$	$NVB$	$VVS$	$VS$	$VVL$	$VVL$	$VL$
	$NB$	$VS$	$M$	$VVL$	$VL$	$M$
	$NM$	$S$	$L$	$VVL$	$L$	$S$
	$AZ$	$S$	$VL$	$VVL$	$VL$	$S$
	$PM$	$S$	$L$	$VVL$	$L$	$S$
	$PB$	$M$	$VL$	$VVL$	$L$	$VS$
	$PVB$	$L$	$VL$	$VVL$	$S$	$VVS$

To improve good performances without precise knowledge of the active power filter parameters, the bandwidth  $HB_k$  is controlled using a fuzzy logic Controller [16] with  $e_k$  and  $\frac{di_{ck}^*}{dt}$  as input variables and  $HB_k$  as the output variable as shown in Fig 3.

In reality, we can take in account the  $DC$  voltage as a third input variable but this can complicate the fuzzy logic controller without a substantial contribution if we suppose that the  $DC$  voltage regulation is correctly achieved.

The fuzzy logic controller is constituted of three principal elements which are: the fuzzification, rule base, and the defuzzification [17].

The fuzzification converts the real values into linguistic size with assigning to each variable a set of fuzzy subsets. For this step, five fuzzy subsets are chosen for  $e_k$ :  $NB$  is negative big,  $NM$  is negative medium,  $AZ$  is almost zero,  $PM$  is positive medium and  $PB$  is positive big (Fig 4(a)). However, in order to increase the dynamic performances of the fuzzy logic controller, seven fuzzy subsets are chosen for the reference current slope:  $NVB$  is negative very big,  $NB$  is negative big,  $NM$  is negative medium,  $AZ$  is around zero,  $PM$  is positive medium,  $PB$  is positive big, and  $PVB$  is positive very big (Fig 4(b)). The universes of discourse of these variables are fixed between -1 and 1 by introducing a simple gain for each variable.

Otherwise, the output variable  $HB_k$  is fuzzed also with seven fuzzy subsets:  $VVS$  is very very small,  $VS$  is very small,  $M$  is medium,  $L$  is large and  $VL$  is very large, and  $VVL$  is very very large (Fig 4(c)). The universe of discourse of the variable  $HB_k$  is fixed between 0 and 1, so, it is necessary to introduce a gain  $G_{HB_k}$  at the fuzzy logic controller output.

Thus, the rule base is expressed as a set of 35  $IF...THEN...$  rules with the use of Mamdani's implication, these rule consigned in the Table 1.

Finally, the defuzzification which gives the real value of the instantaneous hysteresis band is realized by the centroid method.

## 6. Simulation Results

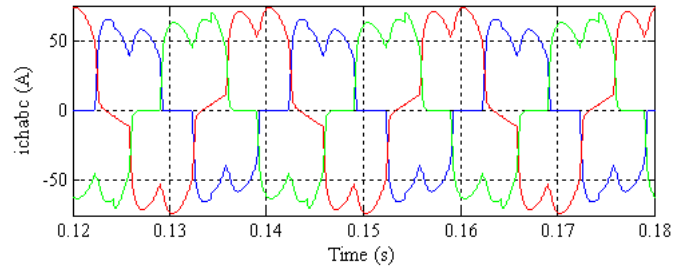
The complete model of the system shown in Fig 1 is implemented and simulated using Matlab/Sumilink. The fuzzy logic controller is established using the Fuzzy Inference System Editor.

The main parameters of the simulated circuit are recapitulated in the Table 2.

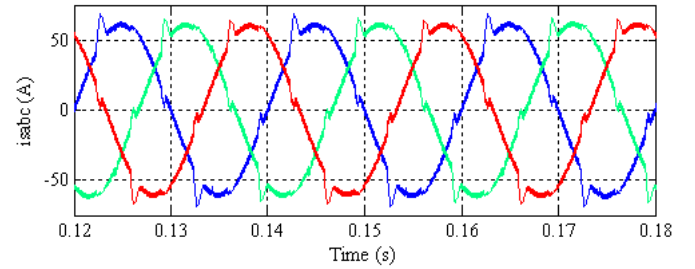
Firstly, we show in Fig 6 and Fig 7 the limits of the conventional PI-control for harmonic compensation. In fact, if the total harmonic distortion ( $THD$ ) is improved, it remains relatively important (about 8% for each phase at the source side). The source current don't presents a good symmetry, this can explain

Table.2. Main parameters of the simulated model.

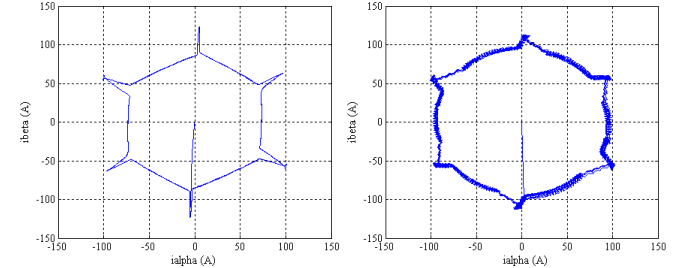
Power Source	230Vrms, 50Hz	
	$R_s = 50m\Omega$	
	$L_s = 0.15mH$	
Non linear Load	<ul style="list-style-type: none"> <li>• Six-pulse current-source converter bridge with a firing angle=15°.</li> <li>• Four-pulse current-source converter bridge between the <math>b</math>-phase and the neutral wire.</li> <li>• Single phase diode bridge between the <math>c</math>-phase and the neutral wire.</li> </ul>	
Active Filter	<ul style="list-style-type: none"> <li>• Capacitors <math>C_1</math> and <math>C_2</math></li> <li>• DC voltages <math>V_{C1}</math> and <math>V_{C2}</math></li> <li>• Inverter side inductance</li> <li>• Switching frequency</li> </ul>	5mF 500V 3mH 10kHz



(a) The three-phase load current.



(b) The three-phase source current.

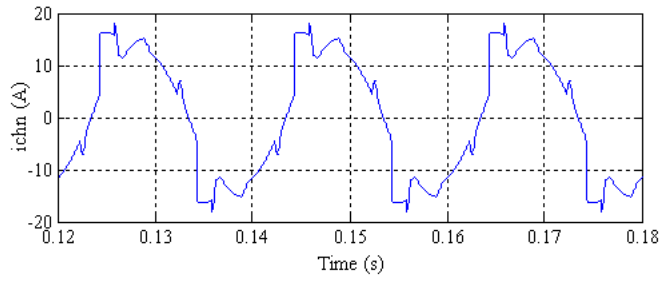


(c) Load current equivalent phasor. (d) Source current equivalent phasor.

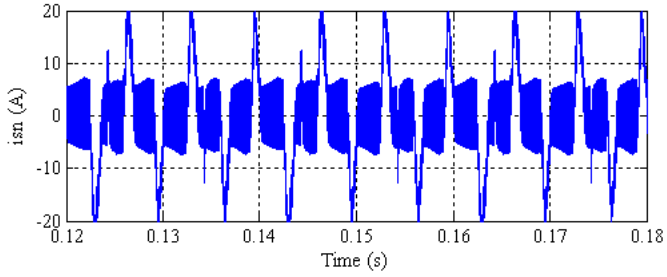
Fig.6. Three-phase current compensation and balance with PI control.

the non total cancelation of the neutral source current as shows Fig 7.

For the proposed control, we present in first time the performances of the fuzzy logic controller are shown in Fig 8. It makes in evidence the advantage of the Fuzzy-hysteresis band controller compared with a conventional fixed bandwidth one. In fact, the Fig 8(a) shows that the variations in instantaneous switching frequency in the case of a fixed bandwidth are important and it is to note that these variations are increasing with decreasing the hysteresis bandwidth. The instantaneous bandwidth established by the fuzzy logic controller is shown in Fig 8(b), and the instantaneous resulting switching frequency in Fig 8(c), we can remark that with varying the instantaneous bandwidth, the instantaneous switching frequency is remained constant around 10kHz. This frequency can be increased or

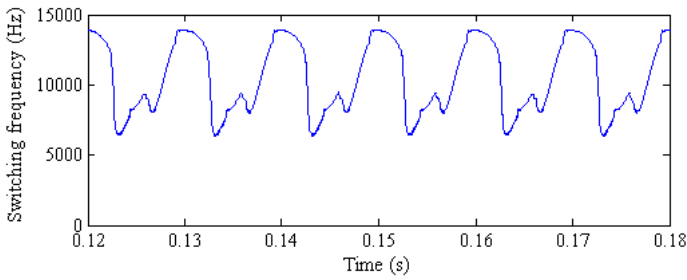


(a) Load neutral current.

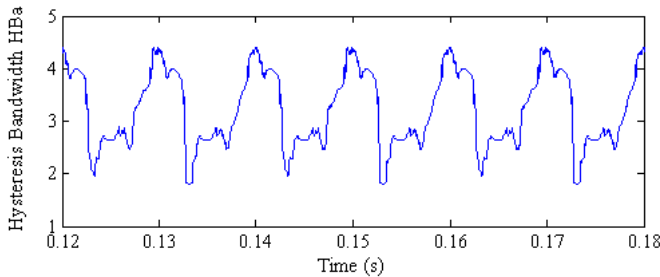


(b) Source neutral current.

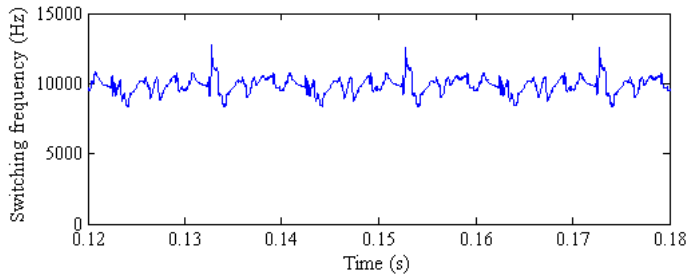
Fig.7. Neutral current compensation with PI control.



(a) Switching frequency (Conventional hysteresis band controller).

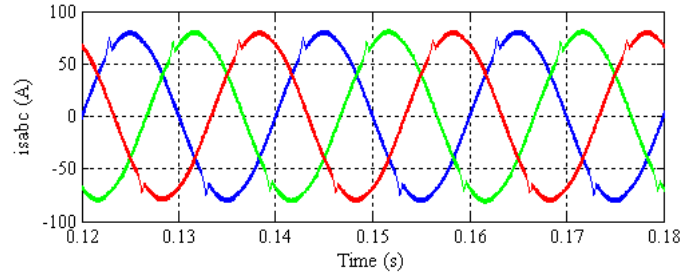


(b) Hysteresis bandwidth (Fuzzy hysteresis band controller).

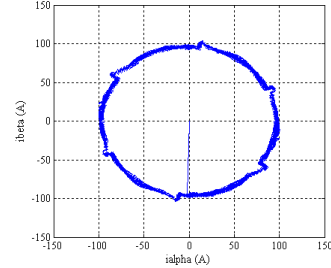


(c) Switching frequency (Fuzzy hysteresis band controller).

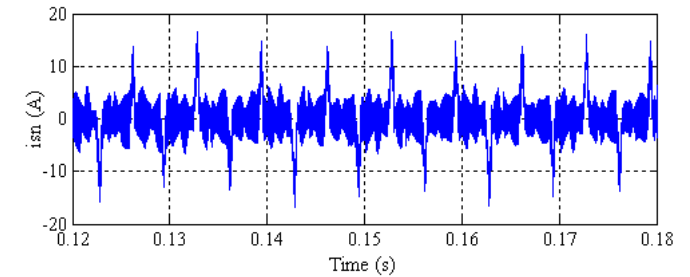
Fig.8. Instantaneous switching frequency of the adaptive Fuzzy-hysteresis band current controller compared with a conventional fixed hysteresis band controller.



(a) The three-phase source current.



(b) Load current equivalent phasor. (d) Source current equivalent phasor.



(c) Source neutral current.

Fig.9. Performances of Fuzzy-hysteresis control on the three-phase and neutral current compensation.

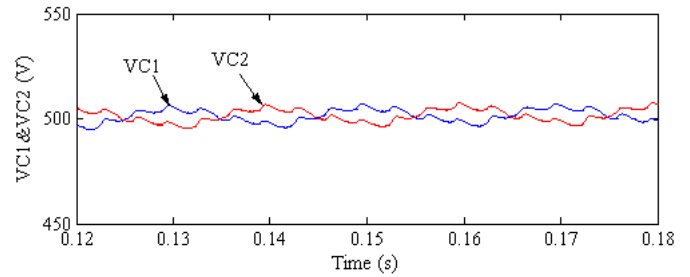


Fig.10. DC Voltage regulation.

decreased by decreasing or increasing the gain at the fuzzy controller output.

The Fig 9(a)(b) illustrate the waveforms of the load and the source current such as there corresponding equivalent phasors in  $(\alpha, \beta)$  coordinate, this figure shows clearly that the harmonics and unbalance are correctly compensated, in fact the unbalance rates are 5% and 0.35% for the load and the source current respectively, therefore, the current in the neutral at source side is almost canceled as shows Fig 9(c).

Otherwise, for the DC voltage control, we can see in Fig 10 that the voltage in the two capacitors are balanced and remained constant.

To show more clearly the performances of the proposed control, Fig 11 represents the harmonics spectrum of the load and source currents for each phase, and in Table 3, we resume

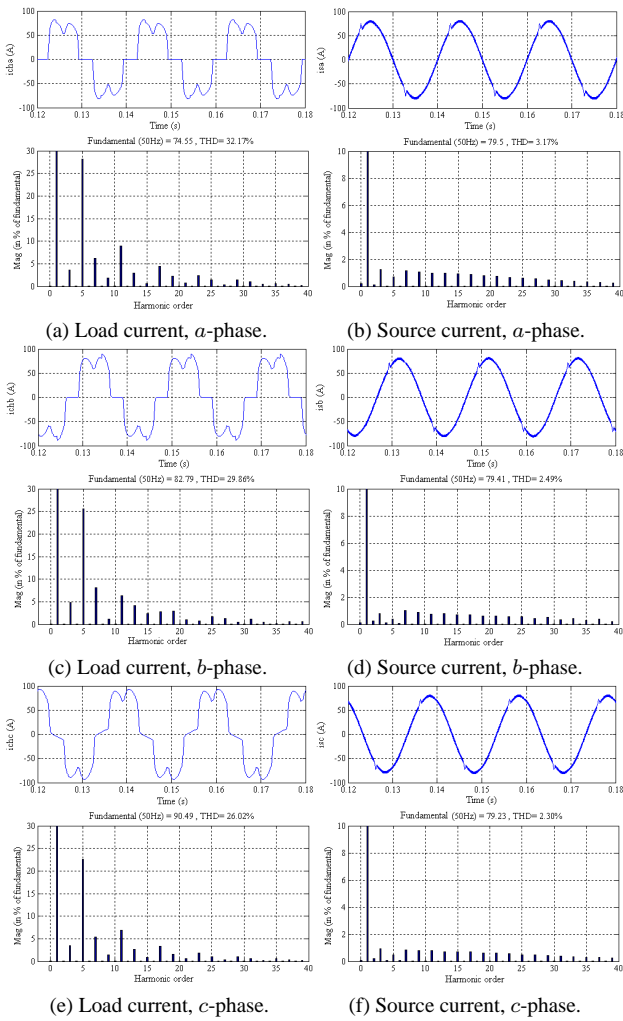


Fig.11. Harmonics current spectrum of the load and source current.

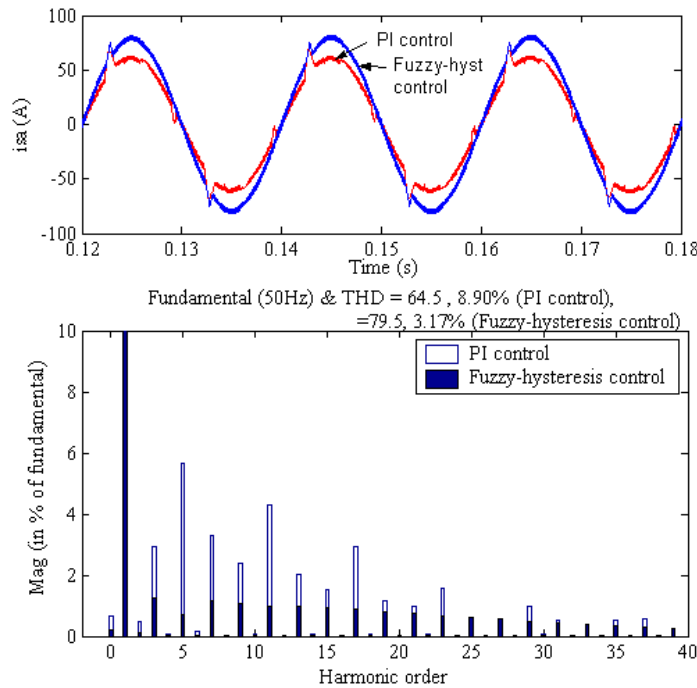


Fig.12. *a*-phase current and its harmonic spectrum with PI control and Fuzzy-hysteresis control.

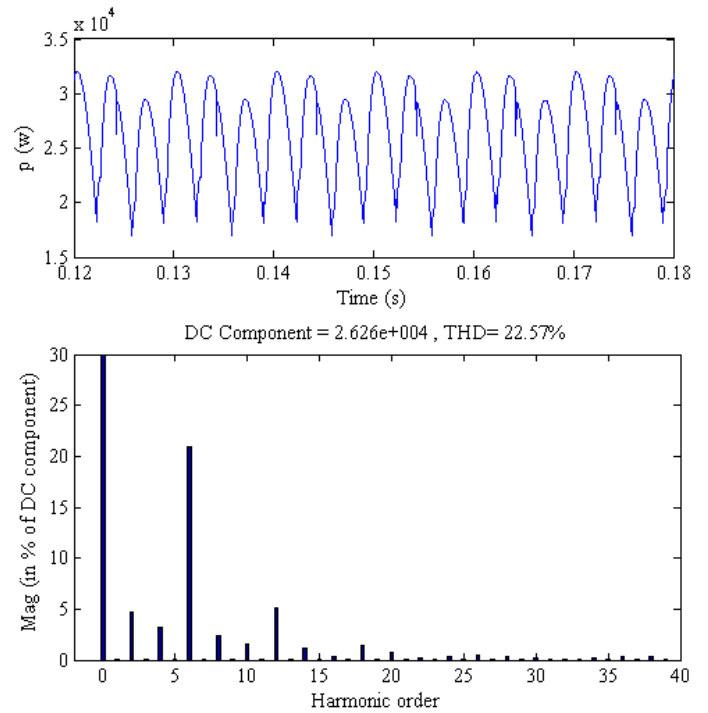


Fig.13. Instantaneous active power and its harmonic spectrum, drawn by the non-linear load.

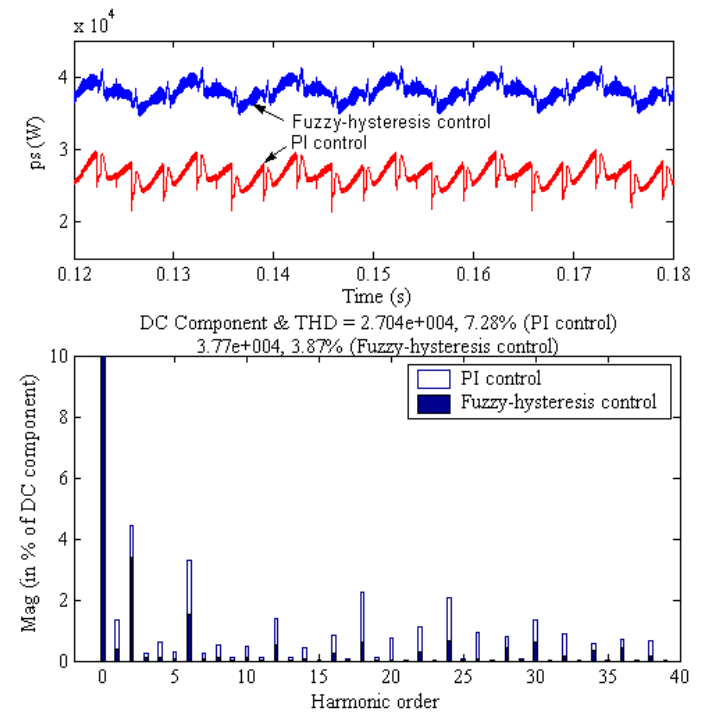


Fig.14. Instantaneous active power and its harmonic spectrum, drawn from the source with the two kinds of control.

the fundamental magnitudes and the total harmonic distortion (*THDs*) for each phase.

In order to make in evidence the comparison between the proposed control with the conventional PI control, we compared the current for the *a*-phase  $i_{sa}$  in Fig 12, and the three-phase instantaneous active power  $p_s$  in Fig 14, at the source side. As it can be seen, the Fuzzy-hysteresis control permits to mitigate almost all harmonics, and to guarantee a best waveform quality improvement of the current, and therefore of the instantaneous

Table.3. Fundamental component and THDs of the load and source current for each phase (Fuzzy-hysteresis control)

Phase	Load current		Source current	
	$I_1$	THD	$I_1$	THD
a-phase	74.55	32.17%	79.50	03.17%
b-phase	82.79	29.86%	79.41	02.49%
c-phase	90.49	26.02%	79.23	02.30%

Table.4. Few main harmonics persisting on the source current and the instantaneous active power, obtained with the two kinds of control.

a-phase current $i_{sa}$			Instantaneous power $p_s$		
h (Hz)	PI control	Fuzzy-hyst control	h (Hz)	PI control	Fuzzy-hyst control
0 (DC)	0.66%	0.18%	0 (DC)	100%	100%
50	100%	100%	50	1.35%	0.37%
150	2.93%	1.23%	100	4.44%	3.38%
250	5.64%	0.69%	300	3.32%	1.51%
350	3.31%	1.15%	600	1.37%	0.53%
450	2.38%	1.09%	800	0.86%	0.27%
550	4.31%	1.00%	900	2.26%	0.63%
THD $_{i_{sa}}$	<b>8.90%</b>	<b>3.17%</b>	THD $_{p_s}$	<b>7.28%</b>	<b>3.87%</b>

active power. In table 4 we have resumed the magnitudes of few main harmonics of the currents  $i_{sa}$  and the power  $p_s$ , all as the total harmonic distortion with the two control kinds.

Note that the THD is calculated at the 40<sup>th</sup> order, and for active power, this one is given to the DC component  $\bar{p}$ .

## 6. Conclusion

In this paper, an adaptive Fuzzy-hysteresis band current controller for four-wire shunt active filter is proposed in order to achieve robust control with a moderate switching frequency. A particular attention was given to compare this controller with a PI one. The Fuzzy-hysteresis controller was firstly described theoretically in detail, to be after verified and validated by simulation. The obtained results for the proposed Fuzzy-hysteresis controller, presents clearly more satisfaction to compensate harmonics and to cancel neutral current, but its principal advantage is that in practical uses, this controller permits to optimize active filter parameters, therefore, to reduce active losses in the passive elements. However, it is important to note that a Fuzzy-hysteresis controller taking in account the DC voltage variations permits to improve the dynamic characteristics of the control and especially the transient state.

## References

- Singh B., Al-Haddad K. and A.Chandra.: *A Review of Active Filters for Power Quality Improvement*. IEEE Transaction on Industrial Electronics, vol. 46, no. 5, October 1999.
- Akagi H.: *Active Harmonic Filters*. Proceeding of the IEEE, Vol.93, No 12, pp 2128-2141. December 2005.
- Afonso J.L., Ribeiro da Silva H.J. and J.S.Martins.: *Active Filters for Power Quality Improvement*. 2001 IEEE Porto PowerTech, ISBN 0 7803 7139 9 Porto 2001.
- Tlust J., Santarius P., Valouch V., Skramlyk J.: *Optimal control of shunt active power filters in multibus industrial power systems for harmonic voltage mitigation*. Mathematics and Computers in Simulation, 71 (2006) 369-376.
- Asiminoaei L., Lascu C., Blaabjerg F., Boldea I.: *Performance Improvement of Shunt Active Power Filter With Dual Parallel Topology*. IEEE Transactions on Power electronics, Vol.22, NO 1, pp 247-259, January 2007.
- Aredes M., Häfner J., Heulmann K.: *Three-Phase Four-Wire Shunt Active Filter Control Strategies*. IEEE Transaction on Power Electronics, Vol12, No.2, pp 311-318 March 1997.
- Ucar M., Ozdemir E.: *Control of a 3-phase 4-leg active power filter under non-ideal mains voltage condition*. Electric Power Systems Research, xxx (2007) xxx-xxx
- Lin B.R., Chiang H.K., Yang K.T.: *Shunt Active Filter with Three-phase Four-Wire NPC Inverter*. The 47th IEEE International Midwest Symposium on Circuits and Systems 2004.
- Alan Gray M.: *A Comparative Analysis of Proportional-Integral Compensated and Sliding Mode Compensated Shunt Active Power Filters*. Master of science thesis, Mississippi State University 2004.
- Etzeberria-Otadui I.: *Sur les Systèmes de l'Electronique de Puissance Dédiés à la Distribution Electrique - Application à la Qualité de l'Energie. (On grid-connected power electronic systems – Power quality improvement application)* PHD thesis, INPG 2003.
- Alali M.A.E.: *Contribution à l'Etude des Compensateurs Actifs des Réseaux Electriques Basse Tension. (Contribution to active compensators study in distribution system)* PHD thesis, Université Louis Pasteur Strasbourg 2002.
- Graovac D., Kati K., Rufer A.: *Unified Power Quality Conditioner Based on Current Source Converter Topology*. EPE, Graz 2001.
- Barbosa Rolim L.G., da Costa D.R., Aredes M.: *Analysing and Software Implimentation of a Robust Synchronizing PLL Circuit Based on the pq Theory*. IEEE Transaction on Industrial Electronics, Vol 53 N° 6 December 2006. pp 1919-1926.
- Lopez de Heredia Bermeo A.: *Commandes Avancées des Systèmes Dédiés à l'Amélioration de la Qualité De l'Energie : de la Basse Tension à la Montée en Tension. (Advanced control of power quality systems : from low voltage to higher voltage)* PDH thesis, INPG 2006.
- Kale M., Ozdemir E.: *An adaptive hysteresis band current controller for shunt active power filters*. Electric Power System Research 73, pp 113-119. 2005.
- Mazari B., Mekri F.: *Fuzzy hysteresis control and parameter optimization of a shunt active filter*. Journal of Information Science and Engineering 21, pp 1139-1156.2005.
- Cirstea M.N., Dinu A., Khor J.G.: *Neural and Fuzzy Logic Control of Drives and Power Systems*. Newnes edition First published 2002.